

Coherent Photoproduction of Eta-Mesons on Spin-Zero Nuclei in a Relativistic, Non-local Model ^{*} [†]

W. Peters[‡], H. Lenske and U. Mosel

*Institut für Theoretische Physik, Universität Giessen
D-35392 Giessen, Germany*

Abstract

The coherent photoproduction of η -mesons on spin-zero nuclei is studied in a relativistic, non-local model, which we have previously applied to the coherent photoproduction of pions. We find that different off-shell extrapolations of the elementary production operator lead to large effects in the cross section. We also show that the almost complete suppression of the $N(1535)$ seen in earlier studies on this reaction is a result of the local or factorization approximation used in these works. Non-local effects can lead to a considerable contribution from this resonance. The relative size of the $N(1535)$ contribution depends on the structure of the nucleus under consideration. We give an estimate for the contribution of the $N(1520)$ resonance and discuss the effect of an η -nucleus optical potential.

PACS numbers: 25.20.Lj, 24.10.Jv

Typeset using REVTeX

^{*}Work supported by BMBF and GSI Darmstadt.

[†]This work forms part of the dissertation of W. Peters.

[‡]Wolfram.Peters@theo.physik.uni-giessen.de

I. INTRODUCTION

Photonuclear reactions offer a unique possibility to test our understanding of hadronic interactions in vacuum as well as in the nuclear environment. For elementary processes like the photoproduction of pions and η -mesons there are sophisticated microscopic models available. These are based on an effective Lagrangian approach and describe the experimental data accurately (see for example [1,2] and references therein). These models provide us with single-particle production operators, needed to treat photonuclear reactions on nuclei in the impulse approximation. Among the numerous possible reactions the coherent photoproduction, in which the nucleus remains in the ground state after the production process, plays a special role: Since the initial and the final state of the nucleus are the same and well understood, the uncertainties with respect to the nuclear structure are less important than in other reactions.

The coherent photoproduction of η -mesons on spin-zero nuclei has experienced renewed interest recently. After work based on a multipole parameterization of the elementary amplitude [3–5], new studies starting from effective Lagrangian models for the elementary process appeared recently [6,7]. One reason for this renewed theoretical effort, apart from the progress made with respect to our understanding of the elementary production, is that in all these works the contribution of the $N(1535)$, which dominates the elementary cross section, is found to be strongly suppressed when coherent production on the nucleus is considered. Thus the other contributions, resulting from the Born terms, the $N(1520)$ resonance and the omega exchange, were predicted to be clearly visible in the coherent photoproduction on nuclei.

In all these works the so called local or factorization approximation is used. In this approximation, the momentum of the incoming nucleon is fixed to a certain value, so that the evaluation of the nuclear transition matrix elements is simplified. In the present study we treat the coherent photoproduction of η -mesons in a relativistic non-local model, i.e. we take the dependence of the production operator on the momentum of the incoming nucleon into account. This model has successfully been applied to the coherent photoproduction of pions on nuclei [8].

In the following section we will first give the details of the elementary model. We then describe how the resulting production operator is evaluated in the case of coherent production. In Sec. IV the different contributions to the coherent cross section as well as the properties of the non-local contributions are discussed in detail. The effect of simple η -nucleus optical potentials is shown. We finally summarize our findings in Sec. V.

II. THE MODEL

A. The elementary operator

The Feynman diagrams contributing to the photoproduction of η mesons on a nucleon are shown in Fig. 1. These graphs are constructed from the following interaction Lagrangians:

$$\mathcal{L}_{\eta NN} = -i g_{\eta NN} \bar{\psi}_N \gamma_5 \psi_N \eta$$

$$\begin{aligned}
\mathcal{L}_{\gamma NN} &= -e \bar{\psi}_N \frac{1}{2}(1 + \tau_3) \gamma_\mu \psi_N A^\mu \\
&\quad - \frac{1}{2} e \frac{\kappa_p}{2m_N} \bar{\psi}_N \frac{1}{2}(1 + \tau_3) \sigma_{\mu\nu} \psi_N F^{\mu\nu} \\
&\quad - \frac{1}{2} e \frac{\kappa_n}{2m_N} \bar{\psi}_N \frac{1}{2}(1 - \tau_3) \sigma_{\mu\nu} \psi_N F^{\mu\nu} \\
\mathcal{L}_{\eta NS_{11}} &= -i g_{\eta NS_{11}} \bar{\psi}_N \psi_{S_{11}} \eta + h.c. \\
\mathcal{L}_{\gamma NS_{11}} &= \frac{eg_{\gamma NS_{11}}}{4m_N} \bar{\psi}_{S_{11}} \gamma_5 \sigma_{\mu\nu} \psi_N F^{\nu\mu} + h.c. \\
\mathcal{L}_{\eta ND_{13}} &= \frac{g_{\eta ND_{13}}}{m_\eta} \bar{\psi}_{D_{13}}^\mu \gamma_5 \psi_N \partial_\mu \vec{\eta} + h.c. \\
\mathcal{L}_{\gamma ND_{13}}^{(1)} &= i \frac{eg_{\gamma ND_{13}}^{(1)}}{2m_N} \bar{\psi}_{D_{13}}^\mu \gamma^\nu \psi_N F_{\mu\nu} + h.c. \\
\mathcal{L}_{\gamma ND_{13}}^{(2)} &= \frac{eg_{\gamma ND_{13}}^{(2)}}{4m_N^2} \bar{\psi}_{D_{13}}^\mu \partial^\nu \psi_N F_{\mu\nu} + h.c. \\
\mathcal{L}_{\omega\eta\gamma} &= \frac{eg_{\omega\eta\gamma}}{4m_\eta} \varepsilon_{\mu\nu\rho\sigma} (V^{\mu\nu} F^{\rho\sigma}) \eta \\
\mathcal{L}_{\omega NN} &= -g_{\omega NN}^v \bar{\psi} \gamma_\mu \psi \omega^\mu \\
&\quad - \frac{1}{2} \frac{g_{\omega NN}^t}{2m_N} \bar{\psi} \sigma_{\mu\nu} \psi V^{\mu\nu} \quad , \tag{1}
\end{aligned}$$

with $F_{\mu\nu} = \partial_\mu A_\nu - \partial_\nu A_\mu$ and $V_{\mu\nu} = \partial_\mu \omega_\nu - \partial_\nu \omega_\mu$, where $A_\mu(\omega_\mu)$ denotes the photon (omega) field.

We take the resonance parameters, as well as the ω and nucleon parameters, from [6], where the data for the elementary photoproduction cross section [9] are well reproduced. The corresponding coupling constants are given in Tab. I. In addition, a form factor is introduced at the ωNN -vertex in [6]:

$$F(t) = \frac{\Lambda^2 - m_\omega^2}{\Lambda^2 - t} \quad , \tag{2}$$

with $\Lambda^2 = 1.2 \text{ GeV}^2$, which is also used here.

III. PHOTOPRODUCTION ON THE NUCLEUS

A. The nuclear wave function

The wave functions needed in the following for the bound nucleons are taken from a relativistic mean-field calculation using scalar and time-like vector potentials V_s and V_v ,

respectively:

$$(\not{p} - m - V_v \gamma_0 - V_s) \psi_\alpha = 0 \quad . \quad (3)$$

For the potentials V^v and V^s we assume a Woods-Saxon shape:

$$V(r) = V_i^o \left(1 + e^{\frac{(r-r_i A^{1/3})}{a_i}} \right)^{-1} \quad ; i = v, s \quad . \quad (4)$$

The parameters for these potentials are given in Table II. They were determined such that the separation energies, the root mean square radius of the charge density and the charge form factors of ^{12}C and ^{40}Ca are well reproduced up to a momentum transfer of 3 fm^{-1} [8]. As discussed in [8], nuclear correlations, which are neglected in a mean-field approach, can become important at a momentum transfer larger than 3 fm^{-1} [10].

B. The amplitude for the coherent photoproduction on the nucleus

The elementary model described in Sec. II A together with the single particle nuclear wave functions introduced in the previous section are now used to calculate the cross section for the coherent photoproduction of η mesons on the nucleus. In the impulse approximation (IA) this is done assuming that the production process takes place on a single nucleon, neglecting many-body contributions. Thus one has to evaluate the diagrams in Fig. 1 replacing the wave functions of in- and outgoing nucleons by the bound state wave functions. The resulting amplitude T is then related to the differential cross section for the coherent photoproduction of η mesons via

$$\frac{d\sigma}{d\Omega} = \left(\frac{M_A}{4\pi W} \right)^2 \frac{q_{cm}}{k_{cm}} \frac{1}{2} \sum_\lambda |T^{(\lambda)}|^2 \quad , \quad (5)$$

where M_A is the mass of the nucleus, k_{cm} and q_{cm} denote the three-momentum of the photon and the η , respectively, in the cm-frame. The total cm-energy is denoted by W and λ stands for the photon polarization.

Since a bound nucleon is off-shell, the matrix element of the production operator has to be evaluated for kinematical situations different from those in the free case. In our model this is done by calculating the corresponding matrix element with the production operator taken directly from the Feynman diagrams.

We work in position space, since the bound state and scattering wave functions are easily obtained in a position space representation. As an example, the direct diagram involving the $N(1535)$ resonance corresponds in our approach to the following non-local expression:

$$\begin{aligned} T_{S_{11}}^{(\lambda)} &= \sum_{\alpha \text{ occ.}} \int d^3x d^3y \bar{\psi}_\alpha(\vec{x}) \phi_\eta^{(-)*}(\vec{x}) \Gamma_{\eta N S_{11}} G_{S_{11}}(E; \vec{x}, \vec{y}) \Gamma_{\gamma N S_{11}}^\mu \phi_\mu^{(\lambda)}(\vec{y}) \psi_\alpha(\vec{y}) \\ &= \sum_{\alpha \text{ occ.}} \int d^3x d^3y \bar{\psi}_\alpha(\vec{x}) \phi_\eta^{(-)*}(\vec{x}) \hat{T}_{S_{11}}^{(\lambda)}(E; \vec{x}, \vec{y}) \phi_\gamma(\vec{y}) \psi_\alpha(\vec{y}) \quad . \end{aligned} \quad (6)$$

Here ψ_α is the wave function of the bound nucleon. $\phi_\mu^{(\lambda)} = \varepsilon_\mu^{(\lambda)} \phi_\gamma$ is the wave function of the photon, where ϕ_γ is a plane wave. $\phi_\eta^{(-)}$ is the wave function of the η satisfying incoming

boundary conditions [11]. $\Gamma_{\eta NS_{11}}$ and $\Gamma_{\gamma NS_{11}}^\mu$ are the vertices resulting from the coupling terms in Eq. (1) and $G_{S_{11}}$ is the resonance propagator:

$$G_{S_{11}}(p_o; \vec{x}, \vec{y}) = \int \frac{d^3 p}{(2\pi)^3} i e^{i\vec{p}(\vec{x}-\vec{y})} \frac{\not{p} + m_{S_{11}}}{p^2 - m_{S_{11}}^2 + im_{S_{11}}\Gamma(p^2)} \quad . \quad (7)$$

The energy dependence of $\Gamma(p^2)$ is taken to be:

$$\Gamma(p^2) = \Gamma_o \left(b_\eta \frac{q_\eta}{q_\eta^o} + b_\pi \frac{q_\pi}{q_\pi^o} + b_{\pi\pi} f(p^2) \right) \quad . \quad (8)$$

For the branching ratios we take $b_\eta = 0.5$, $b_\pi = 0.4$ and $b_{\pi\pi} = 0.1$ and the width is $\Gamma_o = 160$ MeV. q_η (q_π) stands for the three momentum of the η (the pion) in the rest frame of the resonance as a function of its invariant mass p^2 , q_η^o (q_π^o) denote the respective momenta on the mass shell of the resonance. The function $f(p^2)$ fullfils $f(m_{S_{11}}^2) = 1$ and contains the energy dependence of the two-pion decay as given in [12].

The energy E in Eq. (6) is naturally determined by energy conservation:

$$E = E_\gamma + E_\alpha \quad , \quad (9)$$

where E_α is the total, relativistic energy of the bound nucleon.

The resonance propagator depends in position space on \vec{x} and \vec{y} independently, so that the nucleon wave functions in Eq. (6) are evaluated at different positions. This introduces a non-locality in Eq. (6). This non-locality corresponds to a process where a nucleon is taken out of the nucleus at position \vec{y} , and subsequently put back at position \vec{x} . We thus have to calculate a six-dimensional integral; for the technical details we refer the reader to Ref. [8].

For the following discussion it will be useful to rewrite Eq. (6), assuming for the moment the η to be represented by a plane wave:

$$T_{S_{11}}^{(\lambda)} = \int d^3 x d^3 y Tr \left[\hat{T}_{S_{11}}^{(\lambda)}(E; \vec{x}, \vec{y}) \hat{\rho}_A(\vec{y}, \vec{x}) \right] e^{i\vec{k}\vec{y}} e^{-i\vec{q}\vec{x}} \quad . \quad (10)$$

Here $\hat{\rho}_A(\vec{x}, \vec{y})$ denotes the nuclear density matrix in position space:

$$\hat{\rho}_A(\vec{x}, \vec{y}) = \sum_{\alpha \text{ occ.}} \psi_\alpha(\vec{x}) \otimes \bar{\psi}_\alpha(\vec{y}) \quad , \quad (11)$$

which is a non-local quantity. The symbol \otimes denotes the dyadic product of the two spinors. From the local parts $\hat{\rho}_A(\vec{x}, \vec{x})$ of this density matrix, the usual scalar and vector and tensor densities of the nuclear ground state are obtained via:

$$\begin{aligned} \rho_s(\vec{x}) &= Tr[\hat{\rho}_A(\vec{x}, \vec{x})] & \rho_v(\vec{x}) &= Tr[\gamma_o \hat{\rho}_A(\vec{x}, \vec{x})] \\ \rho_t(\vec{x}) \hat{x}_i &= Tr[\sigma^{oi} \hat{\rho}_A(\vec{x}, \vec{x})] \quad . \end{aligned} \quad (12)$$

In [6] and [7], the production operator is treated differently. In both studies the production operator is projected onto a minimal set of Lorentz-covariant operators using the free Dirac equation [2]. In [6] its matrix elements are then evaluated assuming that in the nucleus the relation between small and large components of the nucleon spinors is the same as in

free space. The nuclear structure enters in [6] via empirical parameterizations for the vector form factor of the nucleus. In [7] a different set of Lorentz-covariant operators is used and the nucleon wave functions are taken from a relativistic mean-field calculation like in our model. In this study the production operator is treated relativistically and consists, after the projection procedure, of a tensor, a pseudoscalar and a pseudovector part. In the local approach of [7] it is found, that only the tensor part yields a non-vanishing contribution. Thus in [7] the coherent process only involves the tensor density of the nuclear ground state (Eq. (12)). This will be discussed further in Sec. IV A.

Since both these ways of evaluating matrix elements of the production operator involve the use of on-shell relations, they are equivalent for the η production on a free nucleon, in fact they represent standard techniques used to calculate the elementary process. In the case of off-shell nucleons, however, they lead to different results. Thus, despite of starting from rather similar elementary models, the two works [6] and [7] differ with respect to the off-shell behavior from each other and from our approach. We avoid this ambiguity by taking the production operator directly from the Feynman diagrams, without rewriting it in any way. Thus, we use the natural off-shell behavior of an effective field theory. It must of course be kept in mind, that this also represents an extrapolation of a microscopic model to a kinematical region where it has not been tested against experiment.

The second important difference between [6] and [7] on one side and our approach on the other side is the treatment of the dependence of the production operator on the momenta of the in- and outgoing nucleons. In [6,7] the local or factorization approximation is used, which amounts to putting the momentum \vec{p} of the incoming nucleon equal to a fixed value \vec{p}_o . In order to obtain this approximation, Eq. (6) must be transformed to momentum space. Again we assume the η wave function to be a plane wave:

$$\begin{aligned} T_{S_{11}}^{(\lambda)} &= \sum_{\alpha \text{ occ.}} \int \frac{d^3 p}{(2\pi)^3} \bar{\psi}_\alpha(\vec{p} + \vec{k} - \vec{q}) \Gamma_{\eta N S_{11}} G_{S_{11}}(E; \vec{p} + \vec{k}) \Gamma_{\gamma N S_{11}}^{(\lambda)} \psi_\alpha(\vec{p}) \\ &= \sum_{\alpha \text{ occ.}} \int \frac{d^3 p}{(2\pi)^3} \bar{\psi}_\alpha(\vec{p} + \vec{k} - \vec{q}) \hat{T}_{S_{11}}^{(\lambda)}(E; \vec{p}, \vec{k}, \vec{q}) \psi_\alpha(\vec{p}) \quad , \end{aligned} \quad (13)$$

where we have set $\Gamma_{\gamma N S_{11}}^{(\lambda)} = \Gamma_{\gamma N S_{11}}^\mu \varepsilon_\mu^{(\lambda)}$. In this equation $\vec{k}(\vec{q})$ denotes the three-momentum of the photon (the η). The local approximation now amounts to neglecting the dependence of $\hat{T}_{S_{11}}(E; \vec{p}, \vec{k}, \vec{q})$ on the nucleon momentum \vec{p} . This is done by the replacement $\vec{p} \rightarrow \vec{p}_o$, where \vec{p}_o is independent of the integration variable \vec{p} , and is often assumed to depend on the momentum transfer [8]. Thus one puts:

$$T_{S_{11}}^{(\lambda)} \rightarrow Tr \left[\hat{T}_{S_{11}}^{(\lambda)}(E; \vec{p}_o, \vec{k}, \vec{q}) \hat{\rho}_A(\vec{k} - \vec{q}) \right] \quad , \quad (14)$$

with

$$\begin{aligned} \hat{\rho}_A(\vec{p}) &= \int \frac{d^3 p'}{(2\pi)^3} \sum_{\alpha \text{ occ.}} \psi_\alpha(\vec{p}') \otimes \bar{\psi}_\alpha(\vec{p}' + \vec{p}) \\ &= \int d^3 x e^{i\vec{p}\vec{x}} \sum_{\alpha \text{ occ.}} \psi_\alpha(\vec{x}) \otimes \bar{\psi}_\alpha(\vec{x}) = \int d^3 x e^{i\vec{p}\vec{x}} \hat{\rho}_A(\vec{x}, \vec{x}) \quad , \end{aligned} \quad (15)$$

with $\hat{\rho}_A(\vec{x}, \vec{x})$ being the local part of the nuclear density matrix from Eq. (11). The wave functions of in- and outgoing nucleons are now evaluated at the same position.

We now read off from Eqs. (10), (14) and (15) that the local approximation corresponds in position space to the replacement:

$$\hat{T}_{S11}^{(\lambda)}(E; \vec{x}, \vec{y}) \rightarrow \hat{T}_{S11}^{(\lambda)}(E; \vec{p}_o, \vec{k}, \vec{q}) \delta^3(\vec{x} - \vec{y}) \quad , \quad (16)$$

which is the approximation used in Refs. [6,7]. A similar formula for the local approximation has been given in [13]. This approximation is widely used in DWIA calculations, in a non-relativistic framework its validity has been studied in the photoproduction of charged pions in [14,15].

In this context, the ω -exchange plays a special role. The contribution of the corresponding graph is in our approach given by:

$$\begin{aligned} T_\omega^{(\lambda)} &= \sum_{\alpha \text{ occ.}} \int d^3x d^3y \bar{\psi}_\alpha(\vec{x}) \Gamma_{\omega NN}^\mu \psi_\alpha(\vec{x}) G_{\mu\nu}^\omega(E; \vec{x}, \vec{y}) \Gamma_{\omega\eta\gamma}^{\nu\sigma} \phi_\eta^{(-)*}(\vec{y}) \phi_\sigma^{(\lambda)}(\vec{y}) \\ &= \int d^3x d^3y \text{Tr} [\hat{\rho}_A(\vec{x}, \vec{x}) \Gamma_{\omega NN}^\mu] G_{\mu\nu}^\omega(E; \vec{x}, \vec{y}) \Gamma_{\omega\eta\gamma}^{\nu\sigma} \phi_\eta^{(-)*}(\vec{y}) \phi_\sigma^{(\lambda)}(\vec{y}) \quad , \quad (17) \end{aligned}$$

with $E = E_\gamma - E_\eta$. The important difference between Eq. (17) and Eqs. (6) and (10) is that in the case of the ω -graph, only the local part of the density matrix $\hat{\rho}_A$ appears. In momentum space Eq. (17) reads:

$$\begin{aligned} T_\omega^{(\lambda)} &= \sum_{\alpha \text{ occ.}} \int \frac{d^3p}{(2\pi)^3} \bar{\psi}_\alpha(\vec{p} + \vec{k} - \vec{q}) \Gamma_{\omega NN}^\mu \psi_\alpha(\vec{p}) G_{\mu\nu}^\omega(E; \vec{k} - \vec{q}) \Gamma_{\omega\eta\gamma}^{\nu\sigma} \\ &= \sum_{\alpha \text{ occ.}} \int \frac{d^3p}{(2\pi)^3} \bar{\psi}_\alpha(\vec{p} + \vec{k} - \vec{q}) \hat{T}_\omega^{(\lambda)}(E; \vec{k}, \vec{q}) \psi_\alpha(\vec{p}) \quad . \quad (18) \end{aligned}$$

where we have set $\Gamma_{\omega\eta\gamma}^{\nu\sigma} = \Gamma_{\omega\eta\gamma}^{\nu\sigma} \varepsilon_\sigma^{(\lambda)}$. Due to the appearance of only the local part of the nuclear density matrix $\hat{\rho}_A(\vec{x}, \vec{x})$ in Eq. (17), $\hat{T}_\omega^{(\lambda)}$ does not depend on the nucleon momentum, so that the local approximation has no effect on this amplitude. Consequently, for the omega contribution the different off-shell behavior of the production operator is the main difference between [6], [7] and our model.

C. The eta-nucleus optical potential

It is well known that the production of mesons like pions and η -mesons on the nucleus is strongly affected by the final state interaction between the outgoing meson and the nucleus. While this is neglected in the plane wave impulse approximation (PWIA), it is commonly taken into account in the frame work of the distorted wave impulse approximation (DWIA), by introducing an optical potential, and using scattering wave functions instead of plane waves in Eq. (6). The pion-nucleus interaction is theoretically and experimentally sufficiently well known, while for the η meson there are no data available at all, and we have to resort to theory.

We will show results obtained with the following optical potentials: The optical potential used in [7] is based on the results of [4]. There the η -nucleon scattering amplitude is obtained using a multipole parameterization, which is then used to construct an η -nucleus optical potential via a simple $t\rho$ -approximation.

In [12] the inclusive η -photoproduction is studied using an η self-energy that is based on the model developed in [16]. The corresponding optical potential goes beyond the $t\rho$ -approximation by using an in-medium self-energy for the intermediate $N(1535)$, thus including terms of arbitrary order in the density.

We finally constructed a third optical potential using the results of [17]. Within the models used in this study it was found, that in order to reproduce the data for the inclusive photoproduction of η -mesons, an energy-independent in-medium ηN cross section is needed. For the inelastic ηN cross section a value of 30 mb is given. This can be converted into an optical potential via a $t\rho$ -ansatz, assuming the real part to be zero. We find $-2\omega_\eta V_\eta = i 3 fm^2 p_\eta \rho$, where ω_η is the energy of the η and p_η its three-momentum.

In the following the results of the different optical potentials will be labeled DWIA I, II and III, respectively. The coherent photoproduction treated here might help to obtain more information about the η -nucleus interaction.

IV. RESULTS

In this section the results of our calculations for the coherent photoproduction of η mesons on ^{12}C and ^{40}Ca are discussed in detail. We will also give results for ^4He , despite of the limited applicability of our model for this nucleus. Since there are different aspects to be mentioned for each graph, we will first discuss the differential cross sections for each graph separately, and in the end give results for a complete calculation, with and without an η -nucleus optical potential.

A. The omega graph and the Born terms

In the previous section it has been shown that the present study and [6,7] differ the least in the case of the ω -graph, we therefore start our discussion with this term. Due to the local nature of this graph, the off-shell extrapolation of the production operator is the only difference, the effect of which can be seen in comparison to the results in [6,7].

The ω couples to the nucleon via a vector and a tensor coupling (Eq. (1)). Due to the relative size of the coupling constants and the additional momentum dependence in the case of the tensor coupling, the vector coupling strongly dominates. For a pure vector coupling the Dirac structure of the corresponding production operator is given by a simple vector term (cf. Eq. (18)):

$$\hat{T}_\omega^{(\lambda)} = a_\mu \gamma^\mu \quad (19)$$

with:

$$a_\mu = -ig_{\omega NN}^v G_{\mu\nu}^\omega(E; \vec{k} - \vec{q}) \Gamma_{\omega\eta\gamma}^{\nu(\lambda)} \quad . \quad (20)$$

From this it is clear, that the ω couples directly to the vector density of the nucleus. The omega amplitude then fulfills:

$$\sum_\lambda |T_\omega^{(\lambda)}|^2 = g^2 \frac{k^2 q^2 \sin^2 \theta}{(t - m_\omega^2)^2} |F_v(Q)|^2 \quad , \quad (21)$$

where g is a factor containing the coupling constants and the ωNN form factor. In this equation k and q stand for the three-momentum of the photon and the η -meson, respectively, $Q = |\vec{k} - \vec{q}|$ is the transferred momentum and $F_v(Q)$ is the Fourier transform of the vector density, i.e. the vector form factor:

$$F_v(Q) = 4\pi \int r^2 dr j_0(Qr) \rho_v(r) \quad , \quad (22)$$

where j_0 is the spherical Bessel function of order 0 and ρ_v is the vector density of the nuclear ground state. Thus in our approach the vector coupling of the ω leads to a cross section that is directly proportional to the vector form factor.

This is in line with [6], where the differential cross section is also taken to be proportional to the vector form factor, but it is in contrast to [7]. There the production operator in Eq. (19) is replaced by:

$$\hat{T}_\omega^{(\lambda)} \rightarrow F_T^{\alpha\beta} \sigma_{\alpha\beta} + F_A^\alpha \gamma_5 \gamma_\alpha \quad . \quad (23)$$

The explicit expressions for $F_T^{\alpha\beta}$ and F_A^α are given in [7]. Instead of the vector term in Eq. (19) a tensor and a pseudovector term appear. For the other graphs there is an additional pseudoscalar term, which vanishes in the case of a pure ωNN vector coupling [2]. Due to the local nature of the ω -term, only the tensor term in (23) can contribute to the coherent photoproduction, leading to the tensor form factor in the cross section in [7]. To obtain this tensor term from the original vector structure in Eq. (19), one has to use the free Dirac equation [2]. Thus a production operator of the form (23) is equivalent to the original vector term in Eq. (19) for the photoproduction on a free nucleon, but shows a different behavior if the nucleon is off-shell.

In Fig. 2 we show the differential cross section for the coherent photoproduction of η mesons on ^{12}C at a photon laboratory energy of 650 MeV when only the omega graph is taken into account. This can directly be compared to the results of [6]. Our cross section is about 30 % below the one given there, which we attribute to the different off-shell behavior of the production operator used in [6]. In Fig. 3 we show the corresponding cross section for ^{40}Ca at a laboratory energy of 700 MeV, which can be compared to the results in [7]. Our cross section is about a factor of two lower than the one given there for ^{40}Ca . For ^{12}C a cross section is found in [7] that is larger than ours by an order of magnitude. As discussed in [7], this strong enhancement for ^{12}C is due to the special features of the tensor form factor, to which the differential cross section is proportional in this study. Since in our approach the ω -contribution is governed by the vector form factor, we do not see such an enhancement.

In order to explicitly show that the large differences between our results and those of [7] are due to the different off-shell behavior resulting from the replacement (23), we have performed calculations for the omega graph using the approach from [7] together with our nuclear wave functions and coupling constants. The tensor term in Eq. (23) leads to an ω -contribution similar to Eq. (21), but with the vector form factor replaced by [2,7]:

$$F_v(Q) \rightarrow 2m_N \frac{F_t(Q)}{Q} \quad , \quad (24)$$

where $F_t(Q)$ is the tensor form factor of the nuclear ground state:

$$F_t(Q) = 4\pi \int dr r^2 j_1(Qr) \rho_t(r) \quad . \quad (25)$$

$\rho_t(r)$ is the tensor density defined in Eq. (12). If the nucleon wave function is written as

$$\psi_\alpha(\vec{r}) = \begin{bmatrix} g_a(r) \mathcal{Y}_{J\ell}^M(\Omega_r) \\ i f_a(r) \mathcal{Y}_{J\ell'}^M(\Omega_r) \end{bmatrix} \quad \text{with} \quad \alpha = (a, M), a = (n\ell J) \quad , \quad (26)$$

where $\mathcal{Y}_{J\ell}^M(\Omega)$ is the two component spin angle function, $\rho_t(r)$ is given by:

$$\rho_t(r) = 2 \sum_{a \text{ occ.}} \left(\frac{2J+1}{4\pi} \right) g_a(r) f_a(r) \quad . \quad (27)$$

The results of this calculation are shown in Fig. 4 for a photon energy of 700 MeV in comparison to the results obtained by using our form of the production operator in Eq. (19). Since the two different operators (19) and (23) are equivalent on-shell, it is clear from Fig. 4 that the large differences between our results and [7] are indeed due to the different off-shell behavior of the production operators. Note that the tensor density, being linear in the small component f_a of the nuclear wave function, is very sensitive to the details of the nuclear structure and to relativistic effects, in contrast to the vector density.

Also shown in Figs. 2 and 3 are the results of calculations including in addition the nucleon Born terms. The resulting curves differ very little from the results containing only the omega graph. This is due to the small ηNN coupling constant, and is in agreement with the findings of [6] and [7].

B. The $N(1535)$

The $N(1535)$ resonance strongly dominates the photoproduction of η mesons on a single nucleon. All previous works on the coherent photoproduction of η mesons on nuclei found an almost complete suppression of the $N(1535)$ contribution to the coherent cross section, so that the omega and the $N(1520)$ graphs give the largest contribution. One trivial reason for this suppression is the fact that the $N(1535)p\gamma$ and the $N(1535)n\gamma$ coupling constant have about the same size, but opposite sign (cf. Tab. I), so that in the coherent sum over all bound nucleons there is a large cancellation between the proton and the neutron terms. There is, however, another source of suppression, which is due to the spin structure of the $N(1535)$ -amplitude [4]. In order to study this point, we will now discuss the properties of the contribution of the direct $N(1535)$ -graph to the production operator.

In order to be able to separate local and non-local effects, it is useful to first consider the leading non-relativistic terms in the production amplitude. This is done by dropping the small components of the nuclear wave functions and the intermediate propagator. The term $\hat{T}_{S_{11}}$ defined in Eq. (6) has the explicit form:

$$\hat{T}_{S_{11}}(E; \vec{x}, \vec{y}) = \frac{e g_{\gamma NS_{11}} g_{\eta NS_{11}}}{2m_N} G_{S_{11}}(E; \vec{x}, \vec{y}) \gamma_5 \sigma_{\mu\nu} k^\nu \varepsilon^\mu \quad . \quad (28)$$

In leading non-relativistic order this becomes a 2×2 matrix:

$$\hat{T}_{S_{11}}^{(n.r.)}(E; \vec{x}, \vec{y}) = i \frac{e g_{\gamma N S_{11}} g_{\eta N S_{11}}}{2m_N} (E + m_{S_{11}}) D(E; \vec{x}, \vec{y}) E_{\gamma} \vec{\sigma} \vec{\varepsilon} \quad , \quad (29)$$

where

$$D(E; \vec{x}, \vec{y}) = \int \frac{d^3 p}{(2\pi)^3} \frac{i e^{i\vec{p}(\vec{x}-\vec{y})}}{E^2 - \vec{p}^2 - m_{S_{11}}^2 + i m_{S_{11}} \Gamma(s)} \quad . \quad (30)$$

The occurrence of the $\vec{\sigma} \vec{\varepsilon}$ term in Eq. (29) is a direct consequence of the quantum numbers of the $N(1535)$: Being an S_{11} state, the $N(1535)$ contributes predominantly to the E_{0+} multipole, which is multiplied by $\vec{\sigma} \vec{\varepsilon}$ in the CGLN-form for the elementary production operator [4]. Thus the $N(1535)$ leads in leading non-relativistic order to a production operator that flips the spin of the nucleon.

Now the question arises whether such a spin-flip term can contribute to the coherent photoproduction. In the transition amplitude (6) matrix elements of the production operator are evaluated between nuclear single-particle wave functions with the same quantum numbers. Since the total angular momentum is a good quantum number, a spin-flip operator like the one in (29) can only yield a contribution if the flip of the spin m_s is compensated for by a corresponding change in the orbital angular momentum component m . In closed-shell nuclei such as ^{40}Ca , this compensation is not possible, since all (m, m_s) states are occupied. Thus for such nuclei, the $N(1535)$ does not contribute to the coherent photoproduction of η -mesons, at least in this non-relativistic picture, that ignores spin-orbit effects.

For open-shell nuclei like ^{12}C , however, the above argument no longer holds. As will be shown below, in this case the contribution of the $N(1535)$ depends crucially on whether a local or a non-local treatment is used. Only in the non-local case a spin-flip can be compensated by a change of the orbital angular momentum. The $N(1535)$ is therefore an explicit probe for non-local effects, and its contribution will necessarily be enhanced in a non-local approach, even in a relativistic calculation.

In order to put these arguments on a formal basis, we write the general form of the non-relativistic production operator, which is a 2×2 matrix, in the following way:

$$\hat{T}^{(n.r.)}(E; \vec{x}, \vec{y}) = L + i \vec{K} \vec{\sigma} \quad , \quad (31)$$

where $L = L(E; \vec{x}, \vec{y})$ and $\vec{K} = \vec{K}(E; \vec{x}, \vec{y})$ stand for the spin-non-flip and the spin-flip part of the production operator, respectively. The non-local nuclear density matrix is in leading non-relativistic order also a 2×2 matrix:

$$\hat{\rho}_A^{(n.r.)}(\vec{x}, \vec{y}) = \sum_{a \text{ occ.}} g_a(x) g_a(y) \sum_M \mathcal{Y}_{J\ell}^M(\Omega_x) \otimes \mathcal{Y}_{J\ell}^{M+}(\Omega_y) \quad , \quad (32)$$

where $a = (n\ell J)$, g_a is the radial wave function of the bound nucleon and $\mathcal{Y}_{J\ell}^M(\Omega)$ is the two component spin angle function. For nuclei where all sub-shells (but not necessarily all major shells) are completely occupied it can be shown that [18]:

$$\hat{\rho}_A^{(n.r.)}(\vec{x}, \vec{y}) = \alpha(\vec{x}, \vec{y}) + \vec{\beta}(\vec{x}, \vec{y}) \vec{\sigma} \quad , \quad (33)$$

with

$$\begin{aligned}
\alpha(\vec{x}, \vec{y}) &= \sum_{a \text{ occ.}} \frac{g_a(x)g_a(y)}{4\pi} \left(J + \frac{1}{2}\right) P_\ell(\cos \theta) \\
\vec{\beta}(\vec{x}, \vec{y}) &= i \sum_{a \text{ occ.}} (-1)^{(\ell-J-\frac{1}{2})} \frac{g_a(x)g_a(y)}{4\pi} P'_\ell(\cos \theta) [\hat{x} \times \hat{y}] \quad .
\end{aligned} \tag{34}$$

θ is the angle between $\vec{x} = x\hat{x}$ and $\vec{y} = y\hat{y}$, and P_ℓ and P'_ℓ are the Legendre polynomial of order ℓ and its derivative, respectively. Thus Eq. (10) for the transition amplitude leads in the non-relativistic case to the formula:

$$\begin{aligned}
T^{(\lambda)} &= \int d^3x d^3y \text{Tr} \left[\hat{T}^{(n.r.)}(E; \vec{x}, \vec{y}) \hat{\rho}_A^{(n.r.)}(\vec{x}, \vec{y}) \right] e^{i\vec{k}\vec{y}} e^{-i\vec{q}\vec{x}} \\
&= 2 \int d^3x d^3y (L\alpha + i\vec{K}\vec{\beta}) e^{i\vec{k}\vec{y}} e^{-i\vec{q}\vec{x}} \quad ,
\end{aligned} \tag{35}$$

where L , \vec{K} from Eq. (31) and α , $\vec{\beta}$ from Eq. (33) are functions of \vec{x} and \vec{y} . From its definition in Eq. (34) it is clear, that $\vec{\beta}(\vec{x}, \vec{x}) = 0$. Thus the spin-flip part $\vec{K}\vec{\beta}$ of the production operator does not contribute in a local calculation (cf. Eq. (16)). However, in a non-local calculation the spin-flip part does lead to a non-vanishing contribution via $\vec{\beta}(\vec{x}, \vec{y}) \neq 0$ for $\vec{x} \neq \vec{y}$. The non-spin-flip part L contributes both locally and non-locally.

From the definition of $\vec{\beta}$ in Eq. (34) we can now read off that the size of the non-local effects, arising from the $\vec{K}\vec{\beta}$ -term in Eq. (35), indeed depends on the details of nuclear structure: For a completely occupied shell with given ℓ the two orbitals with different J contribute to $\vec{\beta}$ with a different sign. If spin-orbit effects are neglected, i.e. if the radial wave functions g_a are the same for both orbitals, their contributions to $\vec{\beta}$ cancel exactly, in agreement with the argument we gave above. For a system like ^{12}C , however, where only the $1p_{\frac{3}{2}}$ orbital is occupied and the $1p_{\frac{1}{2}}$ orbital is empty, the contribution of the $1p_{\frac{3}{2}}$ orbital is not cancelled. Since we are using a relativistic equation of motion for the bound states (Eq. (3)), our wave functions contain spin-orbit effects, but the radial wave functions of two orbitals within one shell are still rather similar. The cancellation in $\vec{\beta}$ in the case of a closed-shell nucleus is thus not complete, but this term is still strongly reduced for ^{40}Ca as compared to ^{12}C . Thus there will be a non-local contribution from the $N(1535)$ resonance, which is enhanced for ^{12}C as compared to ^{40}Ca .

Besides this dependence on the nuclear structure non-local effects also lead to a different angular dependence than purely local contributions. The reason is that the non-local parts admix higher multipole components to the transition matrix element. This can be seen by calculating non-local corrections to the local approximation in Eq. (16). This is done by making a Taylor expansion of the production operator $\hat{T}(E; \vec{p}, \vec{k}, \vec{q})$ around a fixed momentum $\vec{p} = \vec{p}_o$ and considering the first order correction to the local approximation. One finds for the transition amplitude (cf. Eq. (14))

$$T^{(\lambda)} = \text{Tr} \left[\hat{T}^{(\lambda)}(E; \vec{p}_o, \vec{k}, \vec{q}) \hat{\rho}_A(\vec{k} - \vec{q}) \right] + \text{Tr} \left[\left(\vec{\nabla}_p \hat{T}^{(\lambda)}(E; \vec{p}, \vec{k}, \vec{q}) \right)_{\vec{p}=\vec{p}_o} \cdot \hat{\rho}_A \right] + \dots \quad . \tag{36}$$

Taking $\vec{p}_o = -\frac{1}{2}(\vec{k} - \vec{q})$, which is similar to the standard choice discussed in [8], $\hat{\rho}_A$ is given by the difference of two dyadic products:

$$\hat{\rho}_A = \frac{i}{2} \sum_{\alpha \text{ occ.}} \int d^3x \left(\psi_\alpha \otimes (\vec{\nabla} \bar{\psi}_\alpha) - (\vec{\nabla} \psi_\alpha) \otimes \bar{\psi}_\alpha \right) e^{i(\vec{k}-\vec{q})\vec{x}} \quad . \tag{37}$$

The spatial derivatives in the first order correction change the angular momentum structure of the matrix element. Inserting the non-relativistic production operator (31) into Eq. (36), the spin-flip part $\vec{K}\vec{\sigma}$ leads to a first order non-local correction that involves a modified nuclear form factor, which for the case of ^{12}C has the form:

$$F_1(Q) = 4\pi \int r dr j_1(Qr) g_{p\frac{3}{2}}^2(r) \quad , \quad (38)$$

where $g_{p\frac{3}{2}}$ is the $1p\frac{3}{2}$ radial wave function and $Q = |\vec{k} - \vec{q}|$ is the transferred momentum. Due to the spatial derivatives in Eq. (36) a spherical Bessel function of first order appears, in contrast to the vector form factor in Eq. (22), which involves spherical Bessel function of order 0. Thus it is apparent, that non-local effects introduce higher multiplicities, in this case a dipole component. In Fig. 5 F_1 is shown in comparison to the vector form factor for ^{12}C . F_1 shows a very different dependence on the transferred momentum than the vector form factor. We can conclude from this difference that the contribution of the $N(1535)$, which is in leading non-relativistic order purely non-local, has a different angular dependence than the omega term, which is proportional to the vector form factor F_v .

In Fig. 6 we show the contribution of the direct $N(1535)$ -graph to the coherent cross section on ^{12}C in a fully relativistic, non-local calculation in comparison to the ω -contribution. The $N(1535)$ -contribution is comparable to the omega term, but shows a very different angular dependence, which is in qualitative agreement with the different Q -dependence of the higher order form factor from Fig. 5 (A photon energy $E_\gamma = 650$ MeV and a scattering angle between 0 and 90° correspond to a momentum transfer between about 1.5 fm^{-1} and 3.5 fm^{-1}).

In Fig. 7 we compare the $N(1535)$ and the omega contributions for ^{40}Ca . For this nucleus the $N(1535)$ yields only a small contribution to the coherent cross section. We thus find that the size of non-local corrections relative to the leading local term is smaller for the closed-shell nucleus ^{40}Ca . In order to show that this is indeed due to a cancellation between the orbitals within one shell, we also show in Fig. 7 the contribution of the $1d\frac{3}{2}$ and the $1d\frac{5}{2}$ -orbital to the $N(1535)$ term separately. The total $N(1535)$ contribution is an order of magnitude below the one of the individual orbitals, in agreement with the argument we gave above. Thus, the relative importance of the $N(1535)$ in the coherent photoproduction is directly affected by the shell structure of the target nucleus. The relative strength shows strong variations when going from closed-shell to closed sub-shell nuclei.

The importance of non-local effects in the coherent photoproduction of η -mesons is a result of the suppression of the $N(1535)$ in a local calculation for this process. Such a suppression does not occur in the inclusive η -photoproduction (see e.g. [12]). In the coherent photoproduction of pions non-local effects are also of minor importance since the Δ yields the dominant contribution in a local as well as in a non-local calculation. Thus only the coherent photoproduction of η -mesons shows a dependence on non-local effects that is strong enough to study these effects in detail.

C. The $N(1520)$

Being a spin- $\frac{3}{2}$ particle, the $N(1520)$ leads to more complicated expressions for the production operator. We take the spin- $\frac{3}{2}$ propagator to be:

$$G_{D_{13}}^{\mu\nu}(p) = i \frac{\not{p} + m_{\Delta}}{p^2 - m_{D_{13}}^2 + im_{D_{13}}\Gamma} \Lambda^{\mu\nu} \quad , \quad (39)$$

with $\Gamma=120$ MeV [6] and

$$\Lambda^{\mu\nu} = \left(g^{\mu\nu} - \frac{1}{3}\gamma^{\mu}\gamma^{\nu} - \frac{2}{3m_{D_{13}}^2}p^{\mu}p^{\nu} - \frac{1}{3m_{D_{13}}}\left(\gamma^{\mu}p^{\nu} - p^{\mu}\gamma^{\nu}\right) \right) \quad . \quad (40)$$

The three-momenta p_i in the last term in Eq. (40) are treated exactly by replacing them with gradient operators in position space and inserting derivatives of wave functions wherever it is necessary. The spatial components of the $p^{\mu}p^{\nu}$ term in Eq. (40) lead to second derivatives, the exact evaluation of which leads to numerical complications. We therefore make the replacement:

$$p_i p_j \rightarrow k_i k_j \quad , \quad (41)$$

where \vec{k} is the photon momentum. This is equivalent to setting the momentum of the incoming nucleon for this particular term to zero, corresponding to a local approximation.

This is unfortunately not the only complication arising for the $N(1520)$ resonance. From Eq. (1) one sees that the second coupling of this resonance to the photon contains the momentum of the nucleon. Thus for the second coupling many more terms arise that contain higher powers of derivatives of wave functions, which would require a rather involved numerical treatment.

For this reason our calculations are restricted to the first kind of coupling of the $N(1520)$ to the photon. In order to interpret our results correctly, one first has to consider the role of the two different couplings to the photon in the elementary photoproduction. For this purpose we show in Fig. 8 the ratio of the isoscalar $N(1520)$ -contribution to the elementary photoproduction of η mesons when both couplings are taken into account and when only the first one is used. The value of this ratio of about 1/20 shows, that using only the first kind of coupling yields a contribution which is about a factor of 20 larger than the one resulting from the inclusion of both kinds of couplings. Thus the total $N(1520)$ -contribution to the photoproduction of η -mesons is the result of a strong cancellation between the two coupling types. Since we only include the first kind of photon coupling of the $N(1520)$, we have to account for this cancellation. This is done in an approximate way by using coupling constants that are rescaled by a factor of $\sqrt{1/20}$. This procedure can only yield a rough estimate, but it allows us to draw qualitative conclusions about the role of the $N(1520)$ in our approach.

In the local calculations of [6,7], the $N(1520)$ contribution is smaller than the one from the omega. In the upper part of Fig. 9 the contribution of the direct $N(1520)$ graph for ^{12}C in our model is shown, together with the other contributions that we discussed above. The $N(1520)$ yields, in the approximation described above, the largest contribution. From the angular dependence we can conclude that this is mainly due to non-local effects, just as in the case of the $N(1535)$ resonance. This is in agreement with the fact that the $N(1520)$ appears in the elementary photoproduction of η -mesons in the E_{2-} and the M_{2-} multipole, which mainly contribute to the spin-flip part of the CGLN-form of the amplitude [4]. That the $N(1520)$ contributes even more than the $N(1535)$ is due to the fact that the isospin averaging

leads to a strong cancellation of proton and neutron contributions in the case of the $N(1535)$ because of the numerical values of its couplings to the photon. This can be seen by extracting the ratio of isoscalar and isovector $N(1535)N\gamma$ and $N(1520)N\gamma$ coupling constants from the values given in Table I. This ratio is given by $g(T=0)/g(T=1) = (g_p + g_n)/(g_p - g_n)$. For the $N(1535)$ we find $g(T=0)/g(T=1) = 0.08$, which means that the $N(1535)N\gamma$ coupling is strongly dominated by an isovector coupling. For the $N(1520)$ we find for its two kinds of coupling to the photon $g(T=0)/g(T=1) = 0.7$ and 1.3 , respectively, so that isoscalar and isovector couplings are of comparable size for this resonance. For $N = Z$ nuclei like ^{12}C and ^{40}Ca with total isospin $T = 0$, the coherent process is almost completely determined by the isoscalar coupling. This isospin selection strongly suppresses the $N(1535)$ contribution, while it affects the $N(1520)$ resonance much less.

In the lower part of Fig. 9 we show the corresponding results for ^{40}Ca . From the non-local character of the $N(1520)$ contribution in the case of ^{12}C it is clear that it contributes less for ^{40}Ca because of the suppression of non-local effects for this nucleus; it turns out to be smaller than the ω -contribution. Thus the differential cross section is for ^{40}Ca still dominated by local contributions, in contrast to the case of ^{12}C , where the size and the shape of the differential cross section is governed by the large non-local contributions of the $N(1535)$ and the $N(1520)$. It must of course be kept in mind, that the $N(1520)$ contribution we find is only an estimate.

D. The complete cross section and the eta-nucleus interaction

After having studied the properties of the single contributions to the coherent photoproduction of η mesons we now discuss the complete cross section. We have performed calculations including the omega graph, the nucleon Born terms, direct and exchange graphs for the $N(1535)$ and the direct $N(1520)$ graph, treated approximately as described in Sec. IV C. In Fig. 9 the resulting differential cross section for ^{12}C and ^{40}Ca at $E_\gamma = 0.65$ GeV is shown, together with the single contributions. For ^{12}C we find a cross section which is at this energy about a factor of three larger than the one in [6] and shows, as has been discussed above, a very different angular dependence. Note that for both nuclei the interference between the local ω -term and the non-local resonance contributions can be both, destructive or constructive, depending on the angle. The reason is that the vector form factor (Eq. (22)), and therefore the ω -amplitude, changes its sign at certain momentum transfers corresponding to the minima in the differential cross section in Figs. 2 and 3. The non-local contributions from the $N(1535)$ and $N(1520)$, that are added coherently to the omega amplitude, do not show such a change in sign, which leads to the interference pattern seen in Fig. 9.

In Fig. 10 we show the differential cross section for ^{12}C for a photon energy of 650 and 750 MeV for a PWIA as well as a DWIA calculation employing the optical potential I which is taken from [7]. At these energies, an η nucleus optical potential mainly leads to an overall decrease of the cross section. In Fig. 11 the corresponding results for ^{40}Ca are shown.

In Fig. 12 we finally show total cross sections for ^{12}C and ^{40}Ca as a function of the photon energy in PWIA and DWIA using the optical potentials I [7], II [12] and III [17]. Due to the different importance of the non-local resonance contributions, the energy dependence of the cross section is not the same for the two nuclei, and the effect of including an optical

potential is slightly different. If only the local ω -contribution is included, both the energy dependence of the total cross section and the effect of an optical potential are very similar for ^{12}C and ^{40}Ca .

One sees from Fig. 12 that the inclusion of an optical potential mainly leads to a decrease of the cross section. All three optical potentials lead to similar results at lower energies, while at higher energies increasing differences are visible. Setting the real part of the optical potential III equal to zero is not a strong assumption, since the real part of potential I and II has only very little influence on the cross section beyond 650 MeV.

In [12] the properties of the $N(1535)$ in nuclear matter are discussed. Using the results of this work we studied the influence of a modification of the $N(1535)$ -properties in the nuclear medium on our results. Employing the model developed in [16], a broadening of the $N(1535)$ by about 30 MeV at normal nuclear density is found in [12]. For the real part of the $N(1535)$ self-energy a potential $V = V_o\rho/\rho_o$ with $V_o=-50\text{MeV}$ is assumed. Analogous to the procedure used in [8] for the Δ -resonance, we include this effectively by changing the mass and the width of the $N(1535)$ by $\delta m=-30$ MeV and $\delta\Gamma=20$ MeV, respectively. The result of such a calculation is shown in Fig. 13. A change of the mass and the width of the $N(1535)$ leads to a shift of strength towards lower photon energies. Due to the smallness of the $N(1535)$ -contribution for ^{40}Ca , the modifications of the $N(1535)$ -properties do not lead to a significant effect for this nucleus.

An experiment has been performed at MAMI, which is currently being analyzed, where the photoproduction of η mesons on ^4He has been measured. The analysis of the experimental data might reveal a coherent signal [19], which could in principle lead to the first data for this process. Although we are aware, that a mean field approximation is only of limited validity for ^4He , we have performed calculations for this nucleus. We find that the form factor of ^4He is reasonably well reproduced for the parameters for the potentials in Eq. (4) also given in Tab. II. The binding energies, however, come out too large. This is a known effect in mean field calculations, related to explicit contributions from many-body correlations [20].

In Fig. 14 we show the complete differential cross section for ^4He as well as the ω -contribution and the contribution from the $N(1520)$ resonance at a photon laboratory energy of 700 MeV. The cross section in Fig. 14 is about a factor of two below the one in [6] and a factor of three smaller than the one given in [7]. The $N(1535)$ contribution is negligible. In the approximation described above the $N(1520)$ contribution is visible, but much smaller than the ω -contribution. We thus find that the coherent η production on ^4He is dominated by the local ω -term. This is easy to understand since ^4He is a closed shell nucleus, so that non-local effects are relatively smaller than in the case of ^{12}C (cf. Sec. IV B). Due to the limited applicability of the mean-field approximation to ^4He , this result can only be considered as a first estimate. The suppression of non-local effects, however, is independent from this uncertainty, since it is a result of the quantum numbers of the ^4He wave functions. Also shown in Fig. 14 is the result of a DWIA calculation. The η -nucleus interaction only leads to a small decrease of the cross section. This is due to the small absorption at a light nucleus like ^4He .

V. SUMMARY AND CONCLUSIONS

We have calculated differential and total cross sections for the coherent photoproduction of η mesons on ^{12}C and ^{40}Ca in a relativistic, non-local model using the impulse approximation. This model has previously been applied to the coherent photoproduction of pions on nuclei, where good agreement with the experimental data was found. Previous calculations for the coherent production of η mesons have used a local approximation and have found a strong suppression of the $N(1535)$ contribution, which dominates the elementary process.

The two main differences between the recent studies [6,7] and our model are the different off-shell extrapolations used for the elementary production operator, and the fact that our calculation contains non-local effects.

We have found a strong dependence of the ω -contribution on the off-shell extrapolation of the production operator, especially in comparison to the approach of [7]. We have also found that non-local effects can lead to a sizable contribution of the $N(1535)$, which shows a different angular dependence than the local ω -contribution. These non-local effects have been shown to depend on the shell structure of the nucleus such that they are small for a closed-shell system like ^{40}Ca , while being strongly enhanced for the open-shell nucleus ^{12}C . The $N(1535)$ is a sensitive probe for these non-local effects, which is a special feature of the coherent photoproduction of η -mesons.

We have given an estimate for the contribution of the $N(1520)$ resonance to the coherent production of η -mesons. This estimate indicates that the contribution of this resonance also contains non-local effects. In the case of ^{12}C , it led to a $N(1520)$ contribution which is even larger than the ω -term. For ^{40}Ca , where non-local effects are smaller, our estimate still yields a sizeable $N(1520)$ -contribution, which is, however, smaller than the omega term.

The large resonance contributions to the coherent production on ^{12}C lead to a resonant behavior of the total cross section for this nucleus. For ^{40}Ca , where the resonances contribute much less due to the relative suppression of non-local effects, the total cross section does not show a resonant behavior. This is in contrast to the coherent production of pions, where the shape of the total cross section for ^{12}C and ^{40}Ca is very similar [8].

Valid conclusions about the applicability of our approach can obviously only be drawn in comparison to experimental data. In view of present experimental attempts to measure the coherent photoproduction of η mesons on ^4He , we also performed calculations for this nucleus, despite of the limited applicability of our model assumptions for such a light system. We have found that the cross section on ^4He is dominated by the local ω -graph.

ACKNOWLEDGMENTS

We gratefully acknowledge helpful discussions with M. Benmerrouche and L.J. Aburaddad. We also would like to thank Thomas Feuster for performing the elementary cross section calculations.

REFERENCES

- [1] Th. Feuster and U. Mosel, *Nucl. Phys.* **A612** (1997) 375.
- [2] M. Benmerrouche, N.C. Mukhopadhyay and J.F. Zhang, *Phys. Rev.* **D51** (1995) 3237.
- [3] V.A. Tryasuchev and A.I. Fiks, *Phys. Atom. Nucl.* **58** (1995) 1168.
- [4] C. Bennhold and H. Tanabe, *Nucl. Phys.* **A530** (1991) 625, *Phys. Lett.* **B243** (1990) 13
- [5] L. Tiator, C. Bennhold, S.S. Kamalov, *Nucl. Phys.* **A580** (1994) 455.
- [6] A. Fix and H. Arenhövel, *Nucl. Phys.* **A620** (1997) 457.
- [7] J. Piekarewicz, A.J. Sarty and M. Benmerrouche, *Phys. Rev.* **C55** (1997) 2571, L.J. Abu-Raddad, J. Piekarewicz, A.J. Sarty and M. Benmerrouche, *Phys. Rev.* **C57** (1998) 2053.
- [8] W. Peters, H. Lenske and U. Mosel, nucl-th 9803009, submitted to *Nucl. Phys. A*.
- [9] B. Krusche et al., *Phys. Rev. Lett.* **74** (1995) 3736.
- [10] F. de Jong und H. Lenske, *Phys. Rev.* **C54** (1996) 1488; H. Müther, G. Knehr und A. Polls, *Phys. Rev.* **C52** (1995) 2955.
- [11] C. J. Joachain, *Quantum collision theory*, 3rd edition, North Holland Physics Publishing, Amsterdam 1983.
- [12] R.C. Carrasco, *Phys. Rev.* **C48** (1993) 2333.
- [13] J.I. Johansson and H.S. Sherif, *Nucl. Phys.* **A575** (1994) 477.
- [14] X. Li , L.E. Wright and C. Bennhold, *Phys. Rev.* **C48** (1993) 816.
- [15] L. Tiator and L.E. Wright, *Phys. Rev.* **C30** (1984) 989.
- [16] H.C. Chiang, E. Oset and L.C. Liu, *Phys. Rev.* **C44** (1991) 738.
- [17] M. Effenberger and A. Sibirtsev, *Nucl. Phys.* **A632** (1998) 99.
- [18] J.W. Negele and D. Vautherin, *Phys. Rev.* **C5** (1972) 1472.
- [19] B. Krusche , *private communication*.
- [20] R. Schiavella, V.R. Pandharipande and R.B. Wiringa, *Nucl. Phys.* **A449** (1986) 219.

TABLES

$g_{\eta NN} = 2.24$	$g_{\eta NS_{11}} = 2.1$	$g_{\eta ND_{13}} = 6.76$
$g_{\omega\eta\gamma} = 0.31$	$g_{\gamma p S_{11}} = 0.73$	$g_{\gamma p D_{13}}^{(1)} = 5.46$
$g_{\omega NN}^v = 10$	$g_{\gamma n S_{11}} = -0.62$	$g_{\gamma n D_{13}}^{(1)} = -0.97$
$g_{\omega NN}^t = 1.59$		$g_{\gamma p D_{13}}^{(2)} = 5.76$
		$g_{\gamma n D_{13}}^{(2)} = 0.66$

TABLE I. Coupling constants used in this study.

Nucleus	V_v (MeV)	r_v (fm)	a_v (fm)	V_s (MeV)	r_s (fm)	a_s (fm)
^{12}C	385.7	1.056	0.427	-470.4	1.056	0.447
^{40}Ca	348.1	1.149	0.476	-424.5	1.149	0.506
^4He	375.7	1.2	0.287	-499.4	1.2	0.287

TABLE II. Strengths, reduced radii and diffusivities for the relativistic scalar and vector mean-field potentials, respectively.

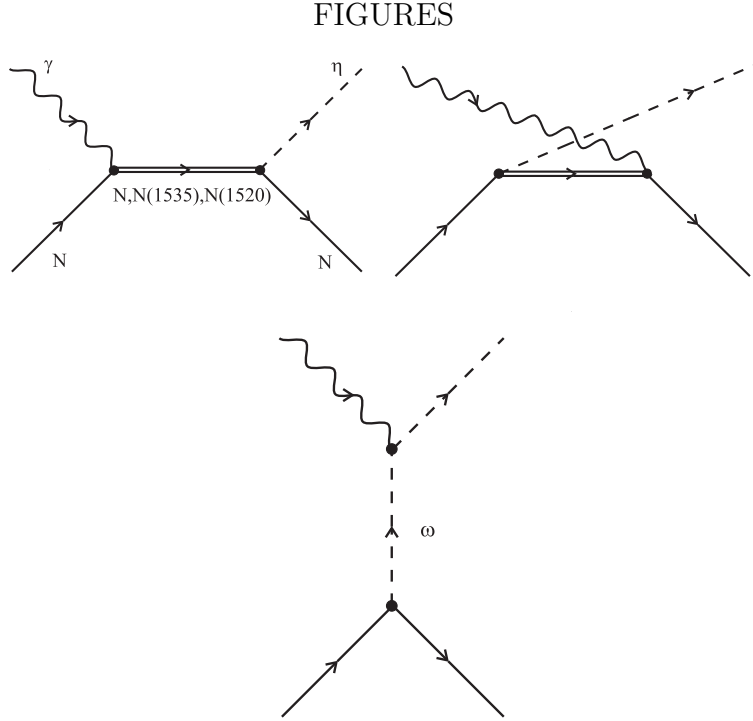


FIG. 1. Feynman diagrams contributing to the photoproduction of η -mesons on a free nucleon.

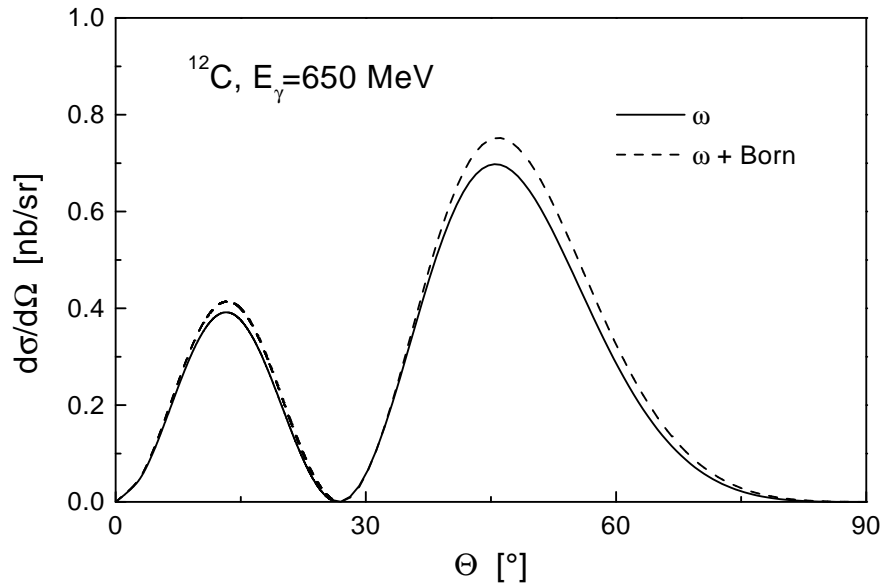


FIG. 2. Differential cross section for the coherent photoproduction of η -mesons on ^{12}C for a photon laboratory energy of 650 MeV resulting from the omega graph and the nucleon Born terms.

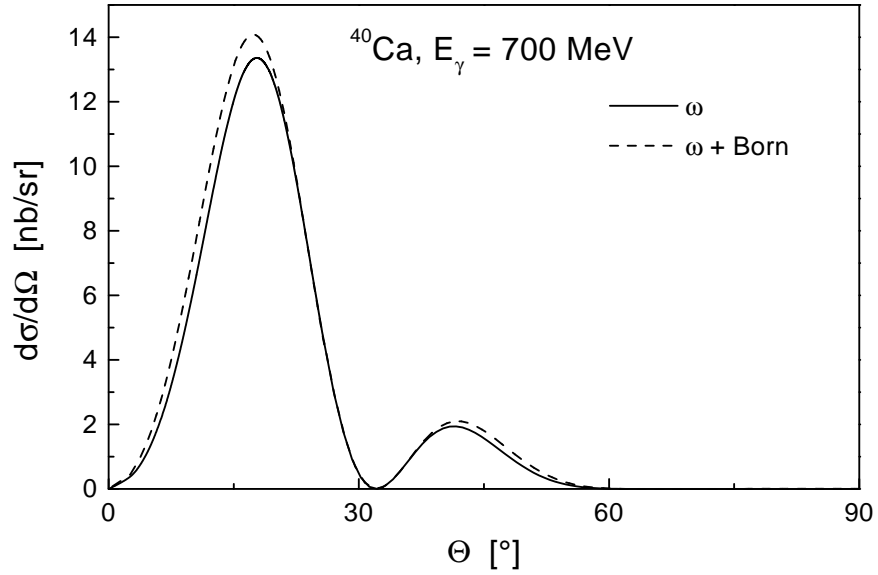


FIG. 3. Differential cross section for the coherent photoproduction of η -mesons on ^{40}Ca for a photon laboratory energy of 700 MeV resulting from the omega graph and the nucleon Born terms.

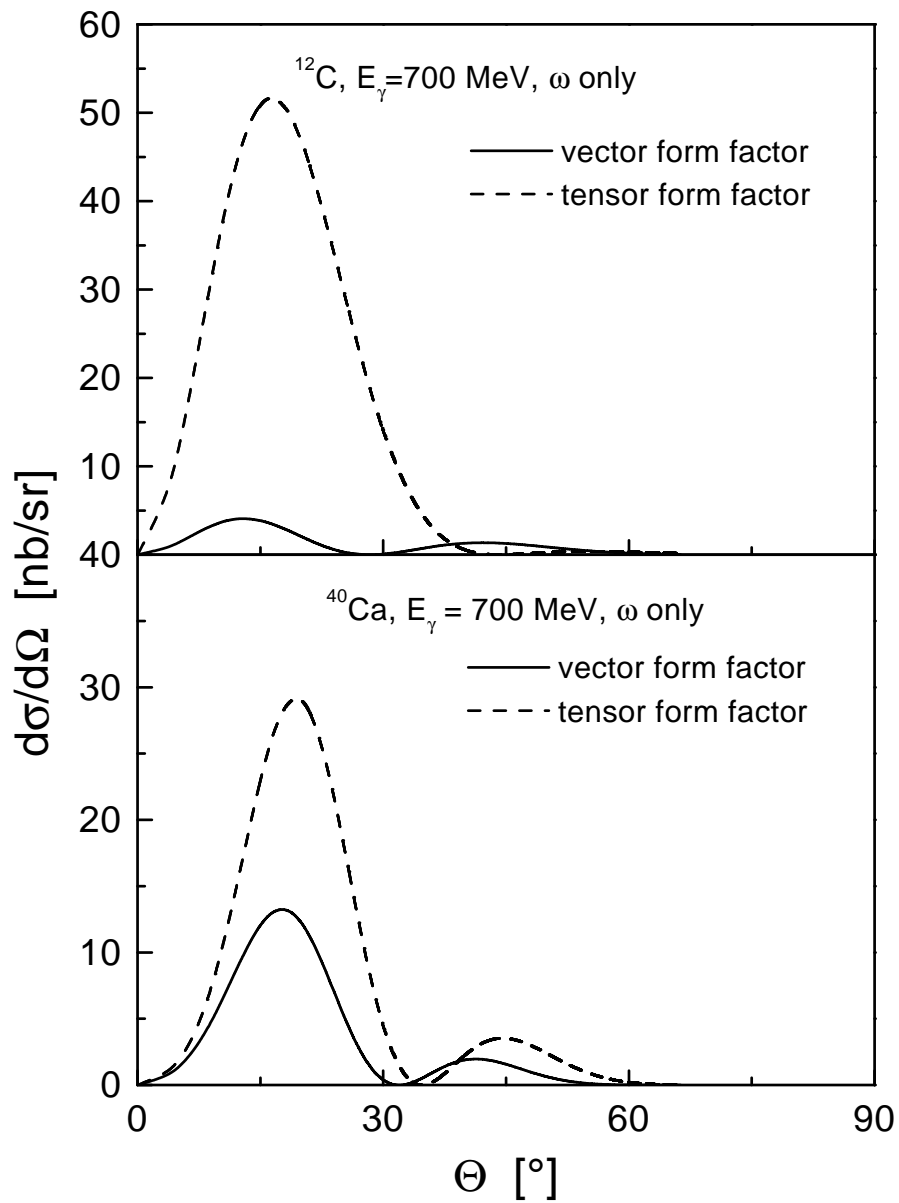


FIG. 4. Differential cross section for the coherent photoproduction of η -mesons for a photon laboratory energy of 700 MeV resulting from the omega graph as in this work (vector form factor) and using the tensor form factor like in [7] as described in the text.

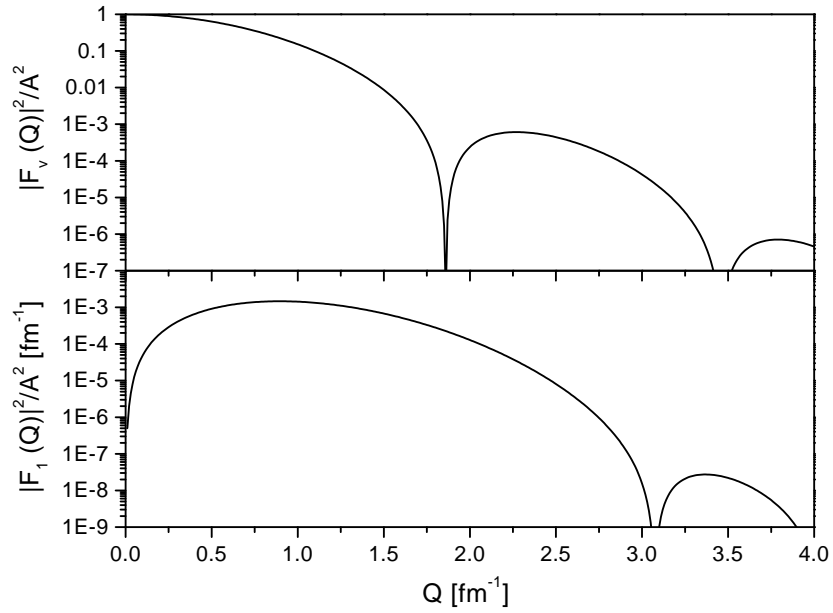


FIG. 5. The vector form factor F_v and the modified form factor F_1 for ^{12}C as defined in the text.

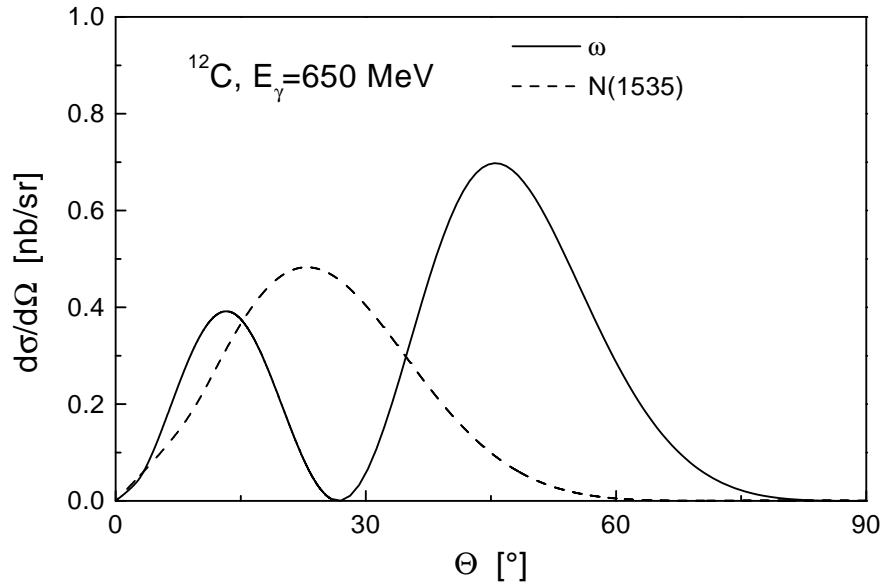


FIG. 6. $N(1535)$ -contribution to the coherent photoproduction of η -mesons on ^{12}C at a photon laboratory energy of 650 MeV in comparison to the omega contribution.

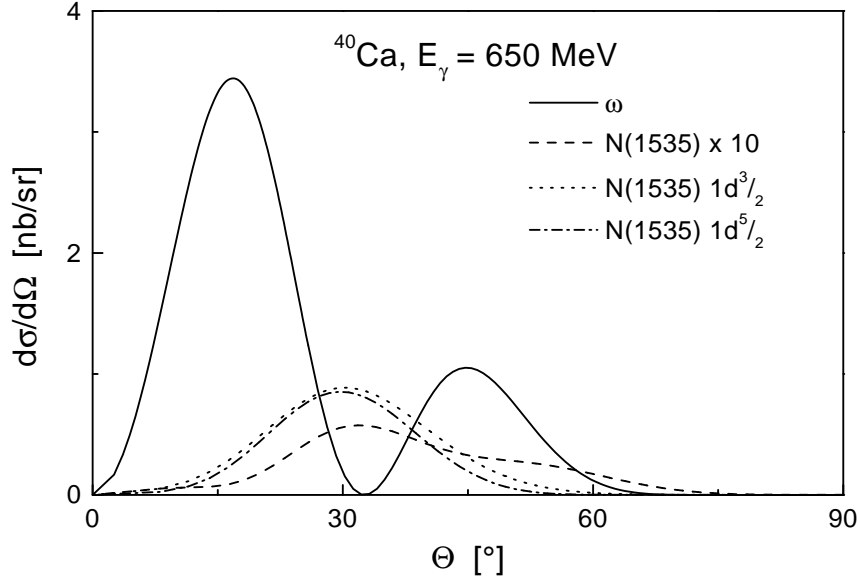


FIG. 7. $N(1535)$ -contribution to the coherent photoproduction of η -mesons on ^{40}Ca at a photon laboratory energy of 650 MeV. The $N(1535)$ -contribution is multiplied by 10. Also shown are the results for the $N(1535)$ -contribution if only the $1d_{3/2}$ and the $1d_{5/2}$ orbital are taken into account.

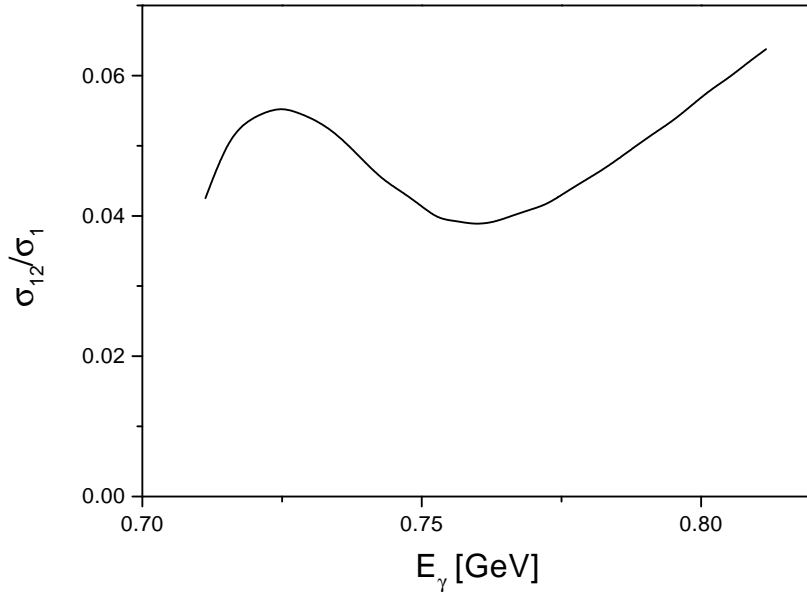


FIG. 8. The ratio of the $N(1520)$ contributions to the isoscalar cross section of the elementary photoproduction of η mesons as a function of the photon energy in the laboratory frame. σ_{12} denotes the entire $N(1520)$ contribution, including both types of couplings to the photon, while σ_1 is the $N(1520)$ contribution when only the first kind of coupling is used.

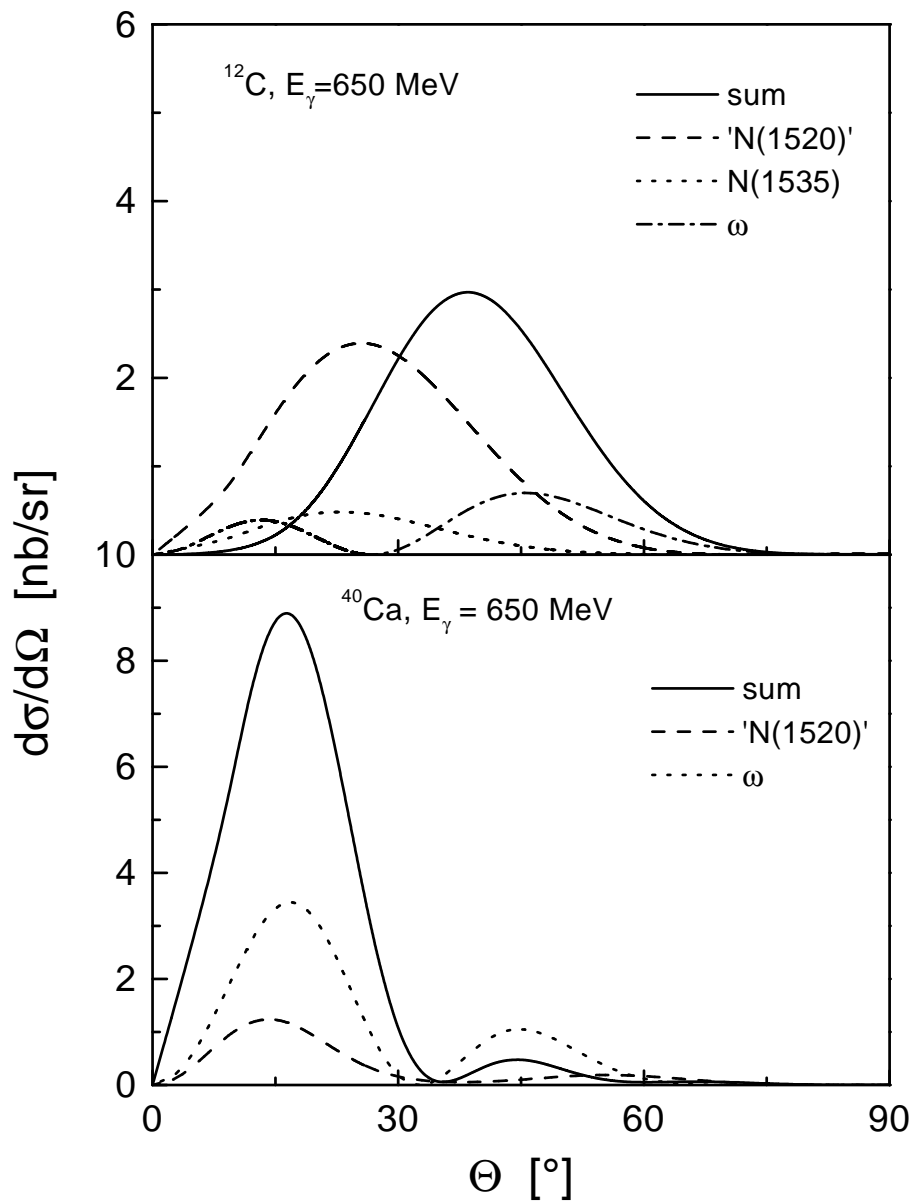


FIG. 9. Complete differential cross section for the coherent production of η -mesons on ^{12}C and ^{40}Ca together with the separate contributions and the estimate of the $N(1520)$ term at a photon laboratory energy of 650 MeV.

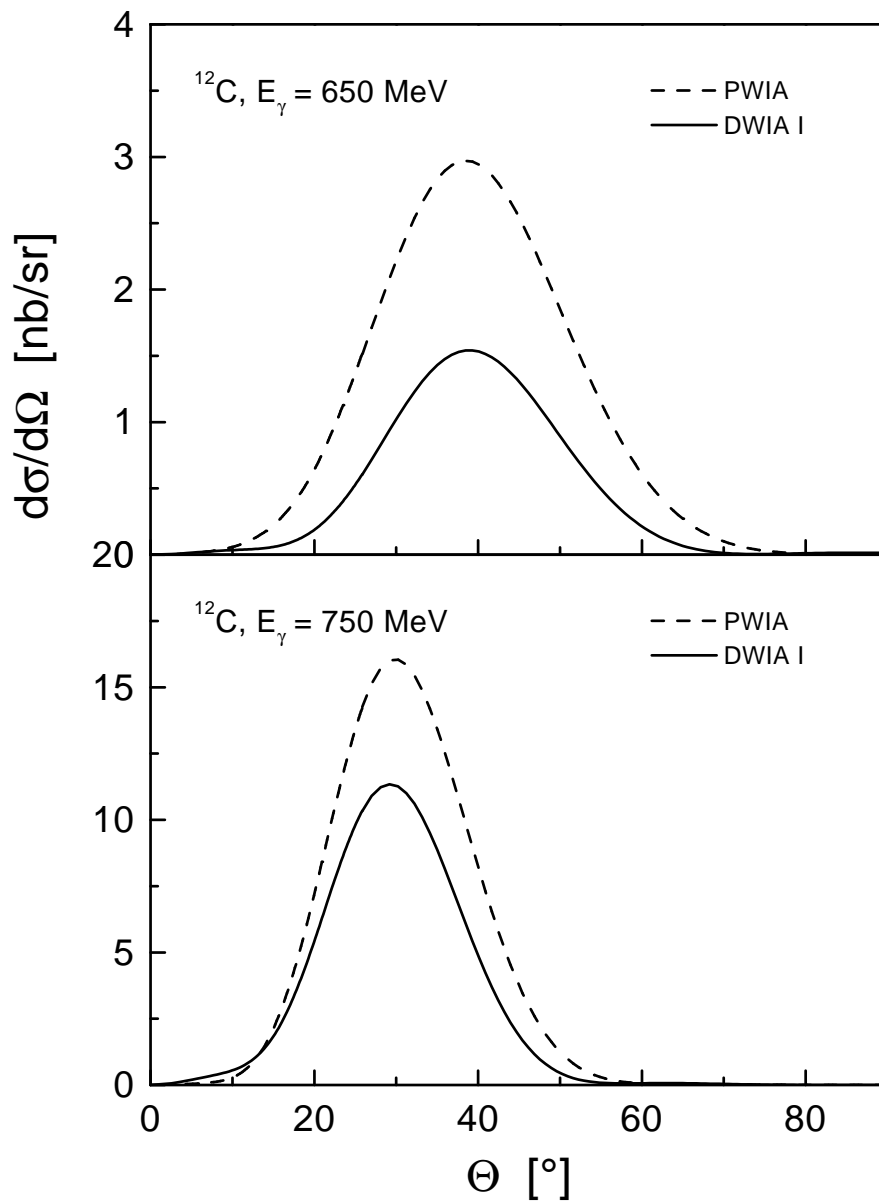


FIG. 10. Differential cross section for the coherent production of η -mesons on ^{12}C for two different photon laboratory energies in PWIA and in DWIA I.

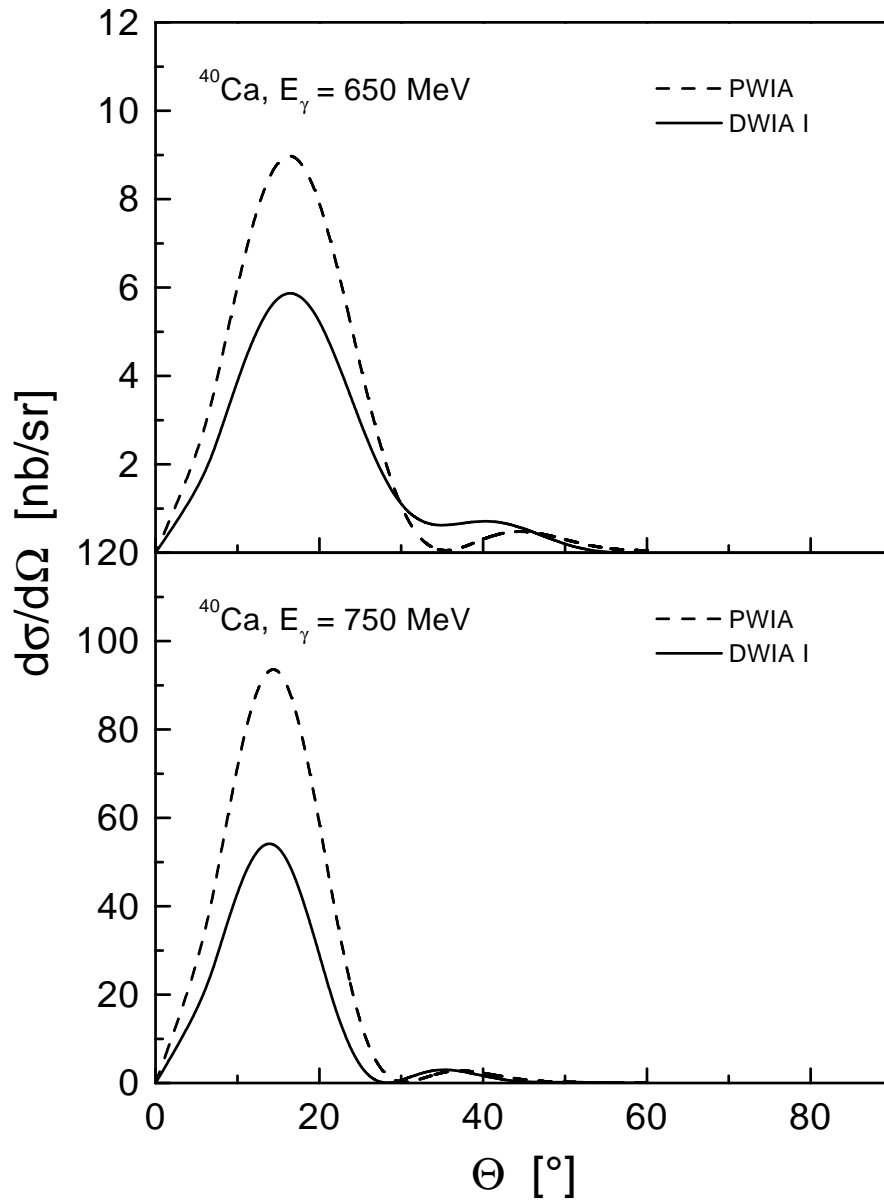


FIG. 11. Differential cross section for the coherent production of η -mesons on ^{40}Ca for two different photon laboratory energies in PWIA and in DWIA I.

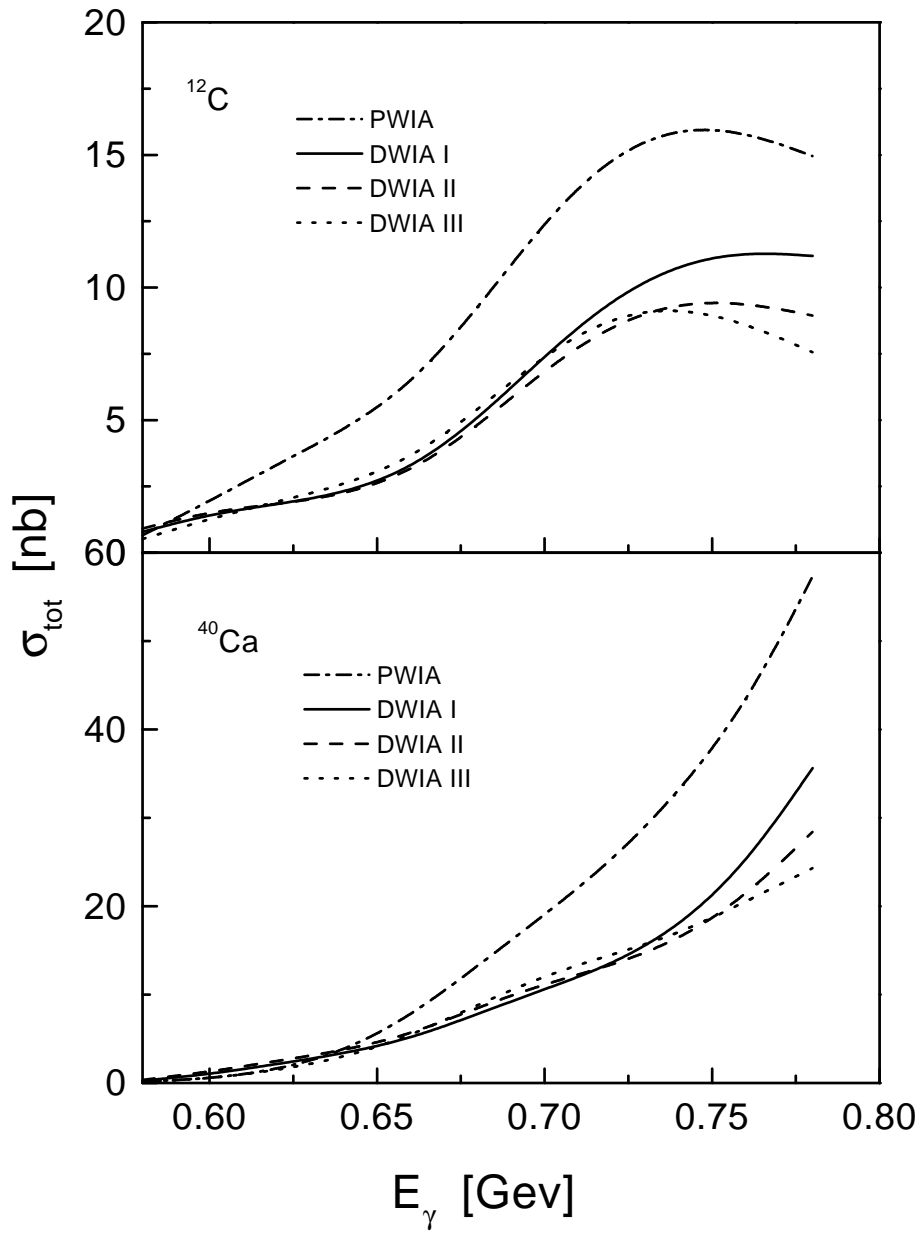


FIG. 12. Total cross section for the coherent production of η -mesons on ^{12}C and ^{40}Ca in PWIA and in DWIA using three different optical potentials as a function of the photon laboratory energy.

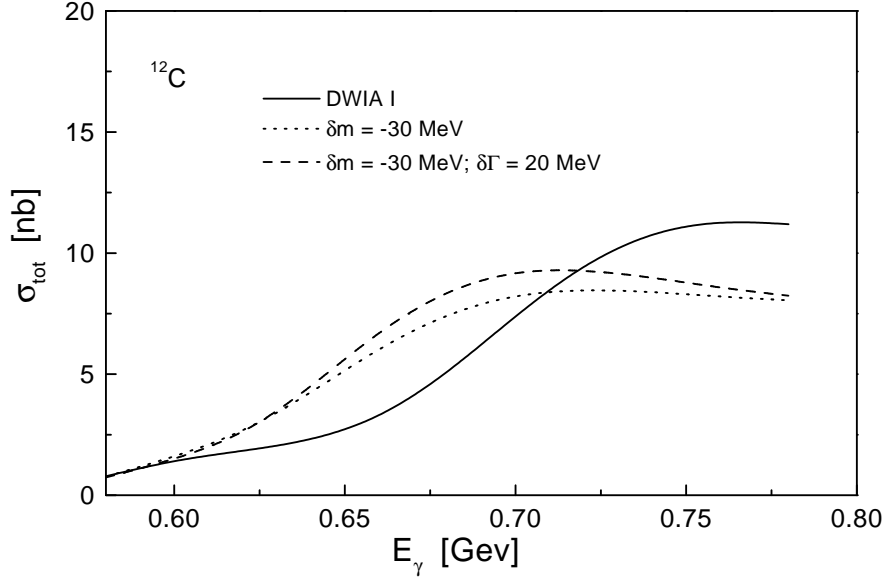


FIG. 13. The effect of a medium modification of the $N(1535)$ as described in the text. Displayed is a calculation where the mass of the $N(1535)$ is changed, as well as one with an additionally modified width, in comparison to a calculation employing the free values.

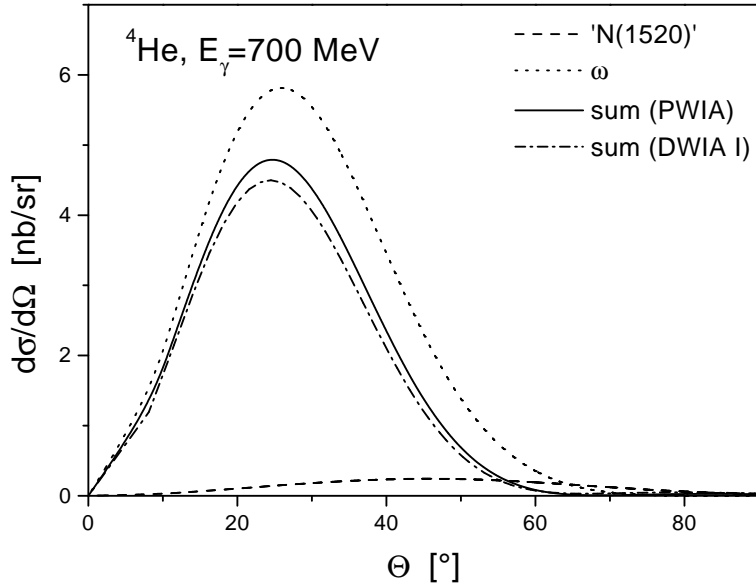


FIG. 14. Differential cross section for the coherent production of η mesons on ^4He at a photon laboratory energy of 700 MeV in a PWIA and a DWIA calculation.